

Oxygen Chemisorption on Cu(110): A Model for the $c(6 \times 2)$ Structure

R. Feidenhans'l, F. Grey, and M. Nielsen

Physics Department, Risø National Laboratory, DK-4000 Roskilde, Denmark

F. Besenbacher, F. Jensen, E. Laegsgaard, and I. Stensgaard

Institute of Physics, University of Aarhus, DK-8000 Aarhus C, Denmark

K. W. Jacobsen and J. K. Nørskov

Laboratory of Applied Physics, Technical University of Denmark, DK-2800 Lyngby, Denmark

R. L. Johnson

II. Institute for Experimental Physics, University of Hamburg, D-2000 Hamburg 50, Federal Republic of Germany

(Received 9 July 1990)

From an interplay between scanning tunneling microscopy, surface x-ray-diffraction experiments, and theoretical predictions, an unequivocal structural model for the Cu(110)- $c(6 \times 2)$ O surface reconstruction is derived with ten Cu atoms within the $c(6 \times 2)$ unit cell, two of which form a Cu *superstructure*. A general picture evolves in which the present as well as the Cu(110)- (2×1) O and the Cu(100)- $(2\sqrt{2} \times \sqrt{2})R45^\circ$ O reconstructions are stabilized by Cu-O-Cu chains directed along the [001] direction. The nucleation and growth of the $c(6 \times 2)$ structure occur preferentially at steps.

PACS numbers: 68.35.Bs, 61.10.-i, 61.16.Di, 68.45.Ax

Oxygen chemisorption on metal surfaces is often accompanied by a large restructuring of the surfaces. Such reconstructions are complex and in general a single experiment or calculation is insufficient to determine the structure. For the oxygen-induced (2×1) reconstruction of Cu(110), for instance, dozens of papers were published supporting various proposed models, until a consensus was recently reached.¹⁻⁵

In the present Letter, we address the question of determining an even more complex structure, the oxygen-induced $c(6 \times 2)$ reconstruction of Cu(110).^{6,7} We shall show how an interplay between surface x-ray-diffraction experiments, scanning tunneling microscopy (STM), and theoretical methods has led to a rather complete understanding of this system. A general picture evolves in which all of the known oxygen-induced reconstructions of copper surfaces, Cu(110)- (6×2) O, as well as Cu(110)- (2×1) O (Refs. 1-5) and Cu(100)- $(2\sqrt{2} \times \sqrt{2})R45^\circ$ O,⁸⁻¹¹ are stabilized by Cu-O-Cu chains along the [001] direction.

We start by a short presentation of the published properties of the Cu(110)- (6×2) O structure. Then our model is presented and the remainder of the paper will basically be a listing of the evidence the different methods give in its favor. The x-ray-diffraction¹² and STM (Ref. 13) results will be discussed in detail elsewhere.

Briefly, the already published information on the $c(6 \times 2)$ structure is the following: (1) About 1 monolayer (ML) of Cu atoms is displaced considerably from the ideal lattice sites.⁷ (2) Two different oxygen-adsorption sites are observed by electron-energy-loss spectroscopy (EELS),¹⁴ one of which has a vibration fre-

quency identical to that for the long-bridge oxygen site observed in the (2×1) phase. (3) The oxygen coverage is $\Theta = 0.90 \pm 0.07$ ML, as reported by high-energy ion scattering⁷ (HEIS) and surface extended x-ray-absorption fine-structure spectroscopy (SEXAFS).¹⁵ Another study, however, concluded that $\Theta = \frac{2}{3}$ ML.¹⁶

The equilibrium structure for the Cu(110)- $c(6 \times 2)$ O reconstruction, which has evolved from our studies, is shown in Fig. 1. Qualitatively, the structure consists of

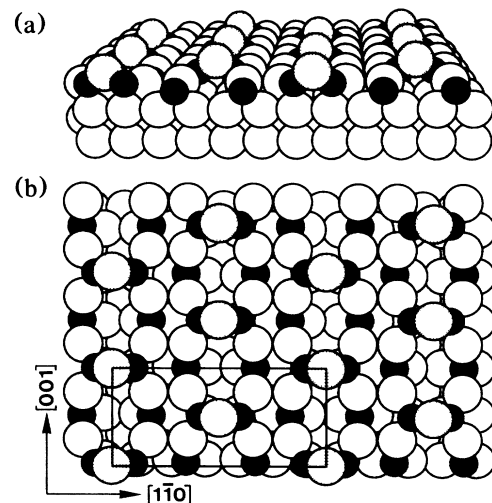


FIG. 1. (a) Perspective and (b) top view of the equilibrium structure for the Cu(110)- $c(6 \times 2)$ O reconstructed phase. The small black circles represent the O atoms, whereas the grey and white circles represent "super" Cu atoms and Cu atoms in the layers below, respectively. A $c(6 \times 2)$ unit cell is shown.

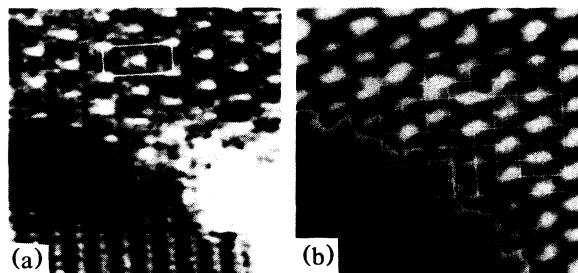


FIG. 2. (a) STM topograph of a $70 \times 70\text{-}\text{\AA}^2$ region showing coexisting phases of $c(6 \times 2)$ highly resolved (top) and (2×1) (bottom). A $c(6 \times 2)$ unit cell is indicated. The height scale from black to white corresponds to 0.66 \AA . (b) Same area; the contrast has been enhanced by applying different grey scales for the two phases. To determine the registry of the $c(6 \times 2)$ protrusions, a net coinciding with the (2×1) protrusions has been superimposed. Surface protrusions are white, while depressions are black.

two Cu-O-Cu chains for each *three* $\langle 110 \rangle$ (1×1) lattice spacings, as compared to the (2×1) structure with only *one* Cu-O-Cu chain per *two* $\langle 110 \rangle$ (1×1) lattice spacings; i.e., the Cu coverage associated with the chains is increased from $\frac{1}{2}$ to $\frac{2}{3}$ ML. The Cu-O-Cu chains are connected by Cu atoms ($\frac{1}{6}$ ML), coordinated to every second O atom along the chain. These Cu atoms, which are gliding on top of the structure, constitute a $c(6 \times 2)$ "superstructure" with respect to the underlying bare (1×1) Cu surface.

The Cu superstructure is directly observable in the high-resolution STM topograph [Fig. 2(a)]. In this case the Cu(110) surface was exposed to $\approx 1.8 \times 10^4$ L ($1 \text{ L} = 10^{-6}$ Torr) oxygen at $\approx 100^\circ\text{C}$, and the (2×1) phase coexists with the $c(6 \times 2)$ phase, which appears as protrusions arranged in a $c(6 \times 2)$ superstructure. This superstructure is rather insensitive to tunneling voltage and current, and the height above the (2×1) reconstruction is $0.6 \pm 0.1 \text{ \AA}$. By following the dynamics of the nucleation and growth of the $c(6 \times 2)$ structure,¹³ it is observed that the individual protrusions are highly mobile along the $[001]$ direction, even at room temperature (RT), which makes the association of the protrusions in Fig. 2(a) with the "super" Cu atoms in the topmost layer highly plausible.

From the STM results, we can also directly conclude that the $c(6 \times 2)$ unit cell contains ten Cu atoms. It was found that the Cu(110)- (2×1) O added-row structure grows on top of terraces by condensation of Cu atoms, supplied from step edges, and O atoms diffusing on the surface.¹⁻³ In the late stages of the formation, rectangular patches with one Cu layer missing appear, which serve as Cu reservoirs for the added rows in the absence of steps. The (2×1) reconstruction is seen both on the terrace and in the patches of Fig. 3(a). Further oxygen exposure leads to a buildup of the $c(6 \times 2)$ structure both on the terrace and within the patches, starting at the

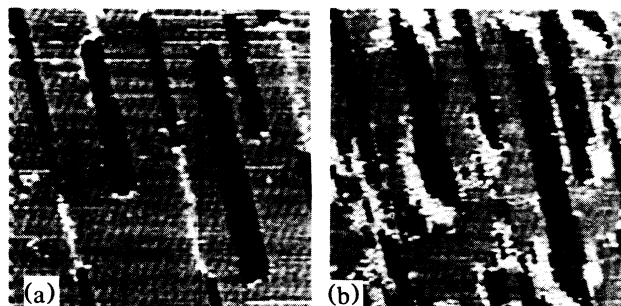


FIG. 3. STM grey-scale topographs over an area of $470 \times 470 \text{ \AA}^2$ showing the nucleation and growth of the $c(6 \times 2)$ reconstructed phase. The surface was imaged while exposed to $\text{O}(2)$ at RT. (a) and (b) correspond to exposures of 400 and 5×10^4 L, respectively. The height scale from black to white corresponds to 2.2 \AA ; the patches are 1.28 \AA lower than the terrace consistent with the interlayer distance, and the $c(6 \times 2)$ structure, which nucleates at the edges both down in the patches and on the terrace, is $\approx 0.6 \text{ \AA}$ higher than the (2×1) structure.

edges, as seen in Fig. 3(b). A simultaneous increase in the size of the patches is observed. Since the (2×1) structure at this point is already fully developed, this additional Cu supply from the patches indicates unambiguously an increased density of Cu atoms in the $c(6 \times 2)$ phase compared to the (2×1) phase. From the change in the areas of the two phases, the amount of Cu supplied from the expanded patches, and a knowledge about the Cu density in the (2×1) phase, the number of Cu atoms within the $c(6 \times 2)$ unit cell is determined to 10 ± 0.5 , corresponding to $\frac{5}{6}$ ML.

Since the Cu superstructure discussed above only contains two Cu atoms per $c(6 \times 2)$ unit cell, eight Cu atoms must be associated with the structure [Fig. 2(a)] underlying the superstructure, and it is difficult to reach a detailed atomic model for the reconstruction based on the STM results alone. However, surface x-ray diffraction is a powerful technique for structural studies of large unit cells.¹⁷

Information about the lateral atomic geometry has been obtained from the Fourier inversion of the in-plane structure-factor intensities, giving the Patterson (auto-correlation) function. A contour plot based on the fractional-order reflections is shown in Fig. 4(a). This gives a map of the interatomic vectors within the unit cell. Apart from the origin, five peaks are clearly observed. Since Cu is much heavier than O, Cu-Cu vectors will dominate the plot. Apart from peak 3, all peaks are at nonsymmetry positions. A model with two nonequivalent Cu atoms [Cu(1) and Cu(2)] is shown in Fig. 4(b). Neglecting peak 4 (which is weak), the model reproduces the main features of the Patterson plot. A least-squares analysis on the fractional-order structure-factor intensities gives $\chi^2 = 12.0$ after refining the displacement of the Cu(2) atoms, an overall Debye-Waller factor, and

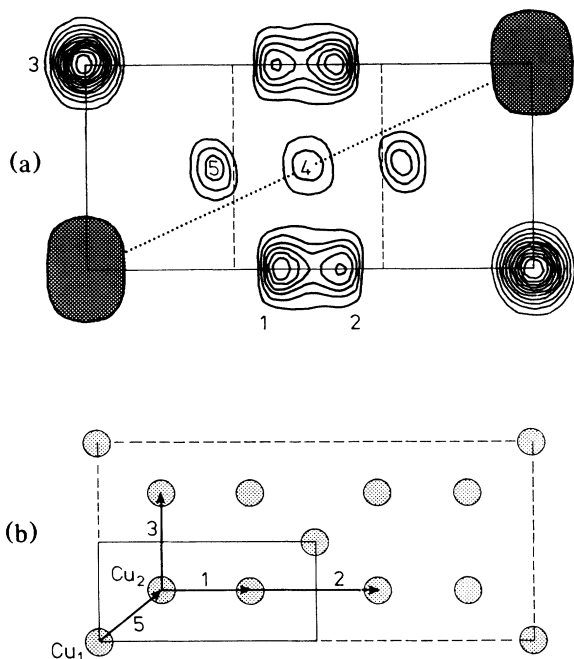


FIG. 4. (a) A contour plot of the Patterson function based on the fractional-order reflections. The corners of the square are (0,0), (3,0), (3,1), and (0,1). The triangle enclosed by the dotted line and two sides is the irreducible unit. The origin is hatched and peaks at twenty contour levels. (b) A model containing two nonequivalent Cu atoms explaining the main features (peaks 1,2,3,5) of the Patterson plot in (a). The dashed rectangle in (b) represents the $c(6 \times 2)$ unit cell (see also Fig. 1), whereas the smaller rectangle in (b) is the rectangle shown in (a), and this smaller one represents only one-quarter of the $c(6 \times 2)$ unit cell.

a scale factor. The Cu atoms will dominate the phases of the structure factors and the O atoms are found in an electron-density difference plot. This highlights the missing part of the structure, i.e., in the O atoms. Two nonequivalent positions are obtained, and the final structure ends up as shown in Fig. 1. The atomic coordinates are refined in a least-squares fit ($\chi^2=1.9$), and the final parameters are given in Table I. From the final structure (Fig. 1) it can be seen that peak 4 in the Patterson contour plot [Fig. 4(a)] is a vector between an oxygen

TABLE I. The atomic positions of the inequivalent atoms for the best fit to x-ray-diffraction results with $\chi^2=1.9$ and as obtained from the total-energy minimization. The coordinates are given with respect to a surface unit cell defined by $\mathbf{a} = [\frac{1}{2}, -\frac{1}{2}, 0]$ and $\mathbf{b} = [001]$.

Atom	Experiment		Theory	
	x	y	x	y
Cu(1)	0.0	0.0	0.0	0.0
Cu(2)	0.890(4)	0.494(3)	0.93	0.50
O(1)	0.689(13)	0.0	0.53	0.0
O(2)	2.009(14)	0.0	1.99	0.0

atom and one of the Cu atoms in the Cu-O-Cu chains.

Returning to the high-resolution STM topograph of Fig. 2(a) we note a detailed structure: two pairs of rows along the [001] direction in between the protrusions. These might be associated with the underlying Cu-O-Cu chains in the model (Fig. 1).

The registry of the model presented in Fig. 1 with respect to the underlying bulk has been derived by both of the experimental techniques. By symmetry the origin of the unit cell, the Cu(1) "superatom" [Fig. 4(b)], can have four possible positions. A comparison to the measured intensity of the integer-order reflections, where the surface and bulk scatter coherently, gave acceptable agreement only for the model shown in Fig. 1; i.e., the Cu atoms of the superstructure are displaced to a short-bridge site between two underlying Cu atoms. This conclusion is confirmed by the STM topograph shown in Fig. 2(b). A grid is placed on the (2×1) protrusions, associated with the O atoms.^{1,3} Extending the grid into the $c(6 \times 2)$ area, the protrusions for $c(6 \times 2)$ Cu superstructure are in registry with the grid positions along the $[1\bar{1}0]$ direction.

The structural model shown in Fig. 1 also results from an effective-medium theory (EMT) total-energy minimization. The approximate nature of the EMT energy expression means that one cannot hope for detailed quantitative comparisons with experiment, but the theory has been shown to give a good account of the half-monolayer oxygen-induced reconstructions on both Cu(110) and Cu(100).⁴

The calculations are performed as in Ref. 4. Of the configurations tried with an oxygen coverage larger than 0.5 ML, the lowest-energy structure found is the one shown in Fig. 1. A similar structure with the "super" Cu atoms missing and the O atoms relaxed back to the Cu-O rows has only a slightly smaller binding energy per oxygen atom. These structures are less stable than the (2×1) structure by 0.1 eV per O atom.

In Ref. 4 it was argued that the driving force behind the oxygen-induced reconstructions of the Cu surfaces is an increased strength of oxygen bonds to Cu atoms with a low coordination number. Lowering the Cu coordination number usually decreases the stability of the atoms, and the "missing-row"-type surface structures are therefore very unstable when clean, but when oxygen is adsorbed, the increase in O-Cu bond strength overcompensates the Cu-Cu binding energy lost. The structure in Fig. 1 (and the other structure mentioned above) represents the highest coverage of Cu-O-Cu rows where all Cu atoms in the rows have lost one neighbor in the first layer. Since the Cu atoms in this structure are less undercoordinated than in the (2×1) structure (where they have all lost two neighbors), the latter is the most stable. The oxygen atoms prefer to sit in the Cu-O-Cu rows in these structures because that allows each of them to bond to two of the undercoordinated Cu atoms.

The "super" Cu atoms in Fig. 1 do not destroy the un-

dercoordination because they are shifted by half a lattice constant along the [001] direction and are thus not nearest neighbors to the Cu atoms along the Cu-O-Cu row. The buckling of the rows comes about due to the possibility of every second O atom to coordinate to the "super" Cu atoms, too. This gives rise to two different kinds of O atoms. Half of them are very much like the O atoms in the (2×1) structure. The calculated vibrational frequency for the mode perpendicular to the surface is 47 meV, very close to that for the (2×1) structure. The "buckled" O atoms give rise to two dipole active vibrational modes with a component perpendicular to the surface. One, which is perpendicular to the plane of the three Cu atoms it coordinates to, is calculated to be 36 meV, and the one parallel to it is 63 meV. This is in good agreement with the EELS experiments,¹⁴ where three losses of 48.5, 41, and 62 meV are observed.

The calculated coordinates are included in Table I. A qualitative agreement with the x-ray data is evident, but the lateral buckling of the O atoms is exaggerated somewhat in the approximate calculation. The "super" Cu atoms are calculated¹⁸ to be 1.2 Å higher than the first Cu layer, and the buckled O atoms are found to be 0.4 Å above the first Cu layer, while the others are 0.2 Å below. The results are also in qualitative agreement with the result of the SEXAFS experiment:¹⁵ Some of the Cu-O distances are different from the (2×1) structure and the difference is larger in the [110] direction than in the [001] direction.

The nucleation and growth of the $c(6\times 2)$ structure will be discussed elsewhere.^{13,19} Very briefly, the $c(6\times 2)$ structure nucleates preferentially at step edges and grows more or less isotropically, as opposed to the (2×1) structure which nucleates at flat terraces and grows anisotropically in Cu-O-Cu added rows.

In conclusion, the proposed structural model incorporates most of the features of the present experiments as well as those published in the literature. This includes the observation by HEIS,⁷ that about 1 ML of Cu atoms are displaced ≥ 0.3 Å away from the ideal lattice sites (in the present model it is $\frac{5}{6}$ ML). The model has an oxygen coverage $\Theta = \frac{2}{3}$ ML in conflict with the HEIS (Ref. 7) and SEXAFS (Ref. 15) experiments ($\Theta = 0.9$ ML), but also $\Theta = \frac{2}{3}$ ML has been reported.¹⁶ To obtain a coverage of 0.9 ML, we need two more oxygen atoms per unit cell. They are, however, not visible in the

electron-density difference plot from the x-ray-diffraction experiment, and in the calculations we tried a number of structures with two extra oxygen atoms, but none had lower energy than the model in Fig. 1.

This work was supported by the Danish Research Councils through the "Center for Surface Reactivity," the Knud Højgaard Foundation, the Max Planck Society, and the Bundesministerium für Forschung und Technologie.

¹D. J. Coulman, J. Wintterlin, R. J. Behm, and G. Ertl, *Phys. Rev. Lett.* **64**, 1761 (1990).

²F. Jensen, F. Besenbacher, E. Lægsgaard, and I. Stensgaard, *Phys. Rev. B* **41**, 10233 (1990).

³F. M. Chua, Y. Kuk, and P. J. Silverman, *Phys. Rev. Lett.* **63**, 386 (1989); Y. Kuk, F. M. Chua, P. J. Silverman, and J. A. Meyer, *Phys. Rev. B* **41**, 12393 (1990).

⁴K. W. Jacobsen and J. K. Nørskov, *Phys. Rev. Lett.* **65**, 1788 (1990).

⁵R. Feidenhans'l, F. Grey, R. L. Johnson, S. G. J. Mochrie, J. Bohr, and M. Nielsen, *Phys. Rev. B* **41**, 5420 (1990).

⁶G. Ertl, *Surf. Sci.* **6**, 208 (1967).

⁷R. Feidenhans'l and I. Stensgaard, *Surf. Sci.* **133**, 453 (1983).

⁸F. Jensen, F. Besenbacher, E. Lægsgaard, and I. Stensgaard, *Phys. Rev. B* **41**, 10233 (1990).

⁹M. Wuttig, R. Franchy, and H. Ibach, *Surf. Sci.* **224**, L979 (1989); **213**, 103 (1989).

¹⁰H. C. Zeng, R. A. McFarlane, and K. A. R. Mitchell, *Surf. Sci.* **208**, L7 (1989).

¹¹I. K. Robinson, E. Vlieg, and S. Ferrer, *Phys. Rev. B* (to be published).

¹²R. Feidenhans'l, F. Grey, R. L. Johnson, and M. Nielsen (to be published).

¹³F. Jensen, F. Besenbacher, E. Lægsgaard, and I. Stensgaard (to be published).

¹⁴J. M. Mundenar, A. P. Baddorf, E. W. Plummer, L. G. Sneddon, R. A. DiDio, and D. M. Zehner, *Surf. Sci.* **188**, 15 (1987).

¹⁵B. Hillert, L. Becker, M. Pedio, and J. Haase, *Europhys. Lett.* **12**, 247 (1990).

¹⁶G. R. Gruzalski, D. M. Zehner, J. F. Wendelken, and R. S. Hathcock, *Surf. Sci.* **151**, 430 (1985); **147**, L623 (1984).

¹⁷R. Feidenhans'l, *Surf. Sci. Rep.* **10**, 105 (1989).

¹⁸This may be a too large outward relaxation as evidenced by a too large buckling of the O atoms, as seen in Table I.

¹⁹D. J. Coulman, J. Wintterlin, J. V. Barth, G. Ertl, and R. J. Behm (to be published).

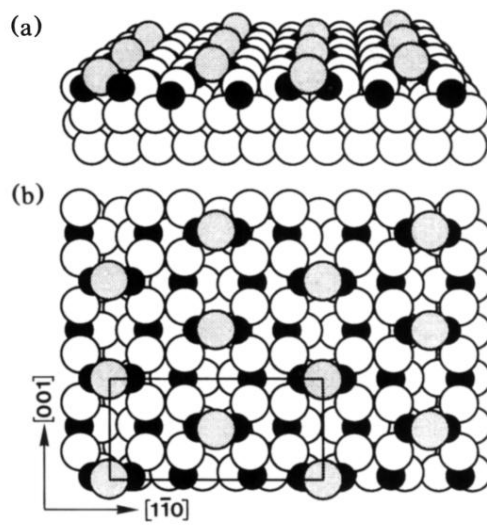


FIG. 1. (a) Perspective and (b) top view of the equilibrium structure for the $\text{Cu}(110)\text{-}c(6\times 2)\text{O}$ reconstructed phase. The small black circles represent the O atoms, whereas the grey and white circles represent “super” Cu atoms and Cu atoms in the layers below, respectively. A $c(6\times 2)$ unit cell is shown.

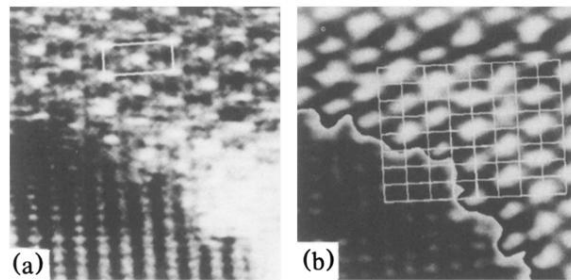


FIG. 2. (a) STM topograph of a $70 \times 70\text{-}\text{\AA}^2$ region showing coexisting phases of $c(6 \times 2)$ highly resolved (top) and (2×1) (bottom). A $c(6 \times 2)$ unit cell is indicated. The height scale from black to white corresponds to 0.66 \AA . (b) Same area; the contrast has been enhanced by applying different grey scales for the two phases. To determine the registry of the $c(6 \times 2)$ protrusions, a net coinciding with the (2×1) protrusions has been superimposed. Surface protrusions are white, while depressions are black.

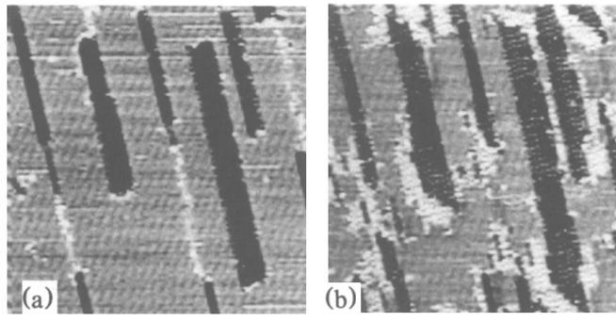


FIG. 3. STM grey-scale topographs over an area of $470 \times 470 \text{ \AA}^2$ showing the nucleation and growth of the $c(6 \times 2)$ reconstructed phase. The surface was imaged while exposed to $\text{O}(2)$ at RT. (a) and (b) correspond to exposures of 400 and 5×10^4 L, respectively. The height scale from black to white corresponds to 2.2 \AA ; the patches are 1.28 \AA lower than the terrace consistent with the interlayer distance, and the $c(6 \times 2)$ structure, which nucleates at the edges both down in the patches and on the terrace, is $\approx 0.6 \text{ \AA}$ higher than the (2×1) structure.

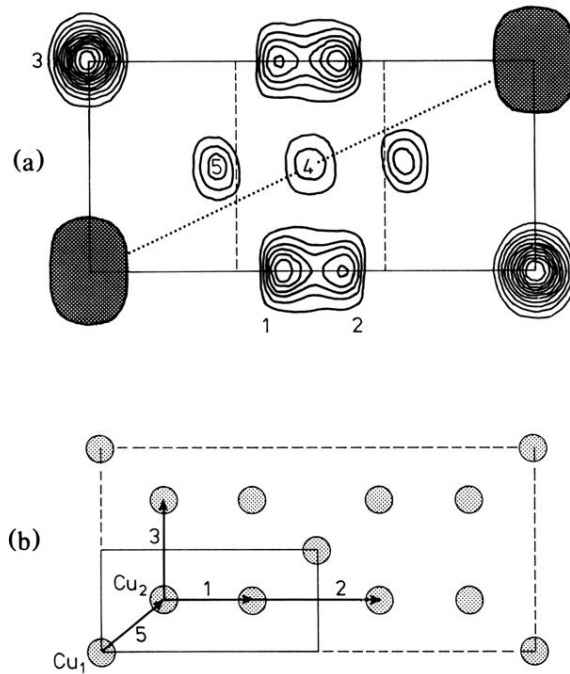


FIG. 4. (a) A contour plot of the Patterson function based on the fractional-order reflections. The corners of the square are $(0,0)$, $(3,0)$, $(3,1)$, and $(0,1)$. The triangle enclosed by the dotted line and two sides is the irreducible unit. The origin is hatched and peaks at twenty contour levels. (b) A model containing two nonequivalent Cu atoms explaining the main features (peaks 1,2,3,5) of the Patterson plot in (a). The dashed rectangle in (b) represents the $c(6 \times 2)$ unit cell (see also Fig. 1), whereas the smaller rectangle in (b) is the rectangle shown in (a), and this smaller one represents only one-quarter of the $c(6 \times 2)$ unit cell.